Colloidal Spheres

DOI: 10.1002/anie.200701355

A Versatile Bottom-up Assembly Approach to Colloidal Spheres from Nanocrystals**

*Feng Bai, Dingsheng Wang, Ziyang Huo, Wei Chen, Liping Liu, Xin Liang, Chen Chen, Xun Wang, Qing Peng, and Yadong Li**

The innovation of bottom-up assembly techniques challenges current lithographic techniques.[1,2] Precise manipulations of small nanocrystal building blocks to construct mesoscopic or macroscopic functional architectures has been the benchmark of nanosciences and nanotechnologies, and provides the possibility of exploiting the size-tunable properties of the integrated macroscopic devices.[3–11] Although a wide scope of superlattices have been fabricated by self-assembly of nanocrystals (NCs), these methods are restricted to the use of mica or silicon plates as substrates.[5–11] The preparation of “soluble” or dispersible aggregates with controllable size, shape, and composition represents a formidable challenge that may lead to the development of strategies for the solution-based synthesis of nanoscale devices.[5–8,11] The development of a general method to prepare dispersible aggregates from nanocrystal building blocks is urgently required. Herein we report a simple and facile microemulsion-based approach for the synthesis of a wide variety of colloidal spheres with different sizes, shapes, and properties by using dispersible NCs as building blocks that consist of, for example, semiconducting metal chalcogenides, metal oxides, and rare-earth compounds. This method is based on a designed oil-in-water (O/W) microemulsion system. The NCs are gathered, assembled, and fixed together spontaneously by the hydrophobic van der Waals interaction of the surfactant ligands absorbed to the NCs during controlled evaporation of a low-boiling oil solvent in the restricted, micrometer-sized 3D space provided by the microemulsion droplets. The size, shape, composition, and surface charge of the colloidal spheres in the size range of 50 nm to 2 μm can be controlled by designed experiment parameters. This approach opens the way to prepare new types of 3D colloid crystals from NCs.

Our basic idea is to use microemulsion oil droplets as confined templates within which the NCs are assembled with the evaporation of low-boiling-point solvents. This approach makes use of two main advantages of oil phases: 1) the low-boiling solvent in the oil phase can be easily removed; 2) since different kinds of solution-phase NC building blocks stabilized by surfactant ligands are well-dispersed in nonpolar oil media with much better phase stability, this method based on O/W emulsion is versatile. The basic processes and principles of the emulsion-based bottom-up self-assembly (EBS) method used in our study are illustrated in Figure 1.

The oil phase containing presynthesized, well-dispersed NCs (0.5–1 %) encapsulated in ligands (oleic acid, octadecyl amine) and the aqueous solution containing different surfactants [cetyltrimethylammonium bromide (CTAB), sodium dodecylsulfate (SDS)] were mixed together with an appropriate oil-to-water ratio (1:5–1:20 by volume). By means of vigorous stirring (greater than 1500 rpm) or ultrasonic treatment, a stable O/W microemulsion system was obtained, in which the well-dispersed NCs were confined in the oil microemulsion droplets that were stabilized by the surfactants present in the aqueous phase. Subsequently, at a chosen temperature, the low-boiling solvent (for example, cyclohexane) was evaporated from the microemulsion system by heat treatment. Through the evaporation of the low-boiling solvent from the oil microemulsion droplets, the droplets shrink and the NCs in the droplets become concentrated and assembled in these confined 3D oil-emulsion droplet spaces. Through the final evaporation of the low-boiling solvents, the NCs stick together to form 3D colloidal spheres. The alkane chains of the surfactants from the aqueous phase spontaneously interdigitate with the alkane chains of the primary ligands located on the outside surface of the assemblies through hydrophobic van der Waals interactions, and the as-obtained colloidal spheres can be well-dispersed in aqueous solution. The products were collected and purified by centrifugation or filtration. By designing proper solution-phase NCs, surfactants, and oil/water two-phase systems and by controlling the emulsion and evaporation processes, a series of 3D colloidal spheres can be assembled from NC building blocks.

We initially chose $BaCrO_4$ nanocrystals as an ideal building block to demonstrate the effectiveness of this approach in assembling 3D colloidal spheres. $BaCrO_4$ NCs (about 6.9 nm) capped with an oleic acid (OA) were synthesized according to previous work.[12,13] In a typical self-assembly approach, a solution of $BaCrO_4$ NCs in cyclohexane (1 mL, about 5 mg mL^{-1}) was added to an aqueous solution (10 mL) of anionic surfactants (SDS, 2.8 mg mL^{-1}) to create an O/W microemulsion by ultrasonic treatment. Then the system was submerged in a heating mantle, and the organic solvent was evaporated at selected temperatures with constant stirring.

---

[*] Dr. F. Bai, D. Wang, Z. Huo, W. Chen, L. Liu, X. Liang, C. Chen,
Dr. X. Wang, Dr. Q. Peng, Prof. Y. Li
Department of Chemistry
Tsinghua University
Beijing, 100084 (China)
Fax: (+86) 10-6278-8765
E-mail: ydli@tsinghua.edu.cn

[**] This work was supported by the NSFC (90606006) and the State Key Project of Fundamental Research (2006CB932300.

Supporting information for this article is available on the WWW under http://www.angewandte.org or from the author.

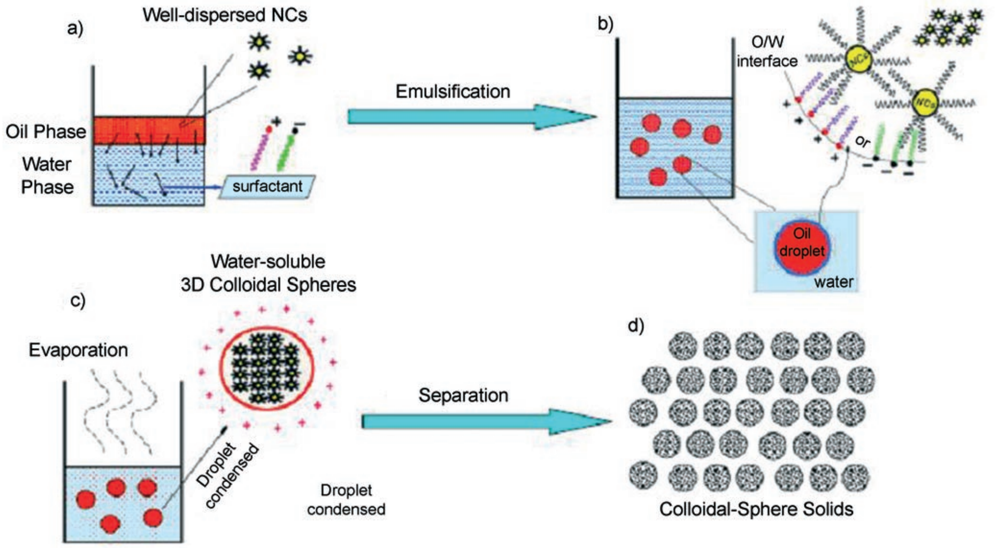

Figure 1. Schematic of the EBS method. a) Mixture of oil phase and water phase (NCs capped with ligands, well-dispersed in cyclohexane, are added to an aqueous solution of surfactant with a volume ratio of 1:5–1:20). b) Formation of the microemulsion system (oil droplets containing NCs are stabilized by surfactant at the interface). c) Evaporation of the low-boiling solvent in the oil droplets at a specified temperature, and the assembly process of the NCs in the confined oil droplets into 3D colloidal spheres, which can be well-dispersed in water. d) Separation of the assembled 3D colloidal sphere solids from the solutions.

Figure 2a shows a TEM image of typical samples of assembled 3D colloidal spheres with sizes in the range of 100–120 nm that were self-assembled from $BaCrO_4$ NCs. These 3D colloidal spheres can self-assemble into ordered 2D arrays on a TEM grid, which indicates that these spherical assemblies may serve as building blocks for more complex colloid assemblies. From HRTEM images of $BaCrO_4$ assemblies (see Figure S2d in the Supporting Information), it is clearly seen that the constituent NCs retain their individual character and do not sinter into larger units. The mean diameter of the $BaCrO_4$ NCs in Figure S2a of the Supporting Information is about 6.9 nm, and the average center-to-center distance between adjacent clusters is about 9.1 nm. These measurements yield an average interparticle gap between clusters of about 2.2 nm, which is smaller than the double thickness of a contracted ligand monolayer (OA 1.7 nm). This phenomenon indicates the presence of chain interdigitation of the ligand layers among adjacent NCs. This result agrees well with the mechanism previously proposed for assembly formation on substrates,[8,10,14] that is, multiple interactions of long-chain alkyl groups arising from long-chain molecule-induced assembly, which stabilizes the complex superstructure system. To confirm that the stable spherical assemblies exist in solution, we chose dynamic light scattering (DLS) to analyze these colloidal spheres. The DLS results show that the hydrodynamic diameters of the spherical assemblies amount to about 120 ± 30 nm for $BaCrO_4$, which agrees with the TEM results. Zeta potentiometer characterization indicates that these colloidal sphere assemblies have a negative surface charge (−27.6 mV; see Figure S2e in the Supporting Information).

To further demonstrate this bottom-up assembly approach, we selected well-dispersed Ag_2Se NCs stabilized with octadecyl amine as representative building blocks with CTAB ($3.6\,mg\,mL^{-1}$) as surfactant. TEM and high-resolution images reveal that Ag_2Se NCs can form well-ordered 3D colloidal spheres by the EBS method. The DLS results show that the spherical assemblies are well-dispersed in the aqueous phase and the hydrodynamic diameters are about 180 ± 60 nm for Ag_2Se. Zeta potentiometer characterizations indicate that these colloidal sphere assemblies have a positive charge (+38.0 mv) with

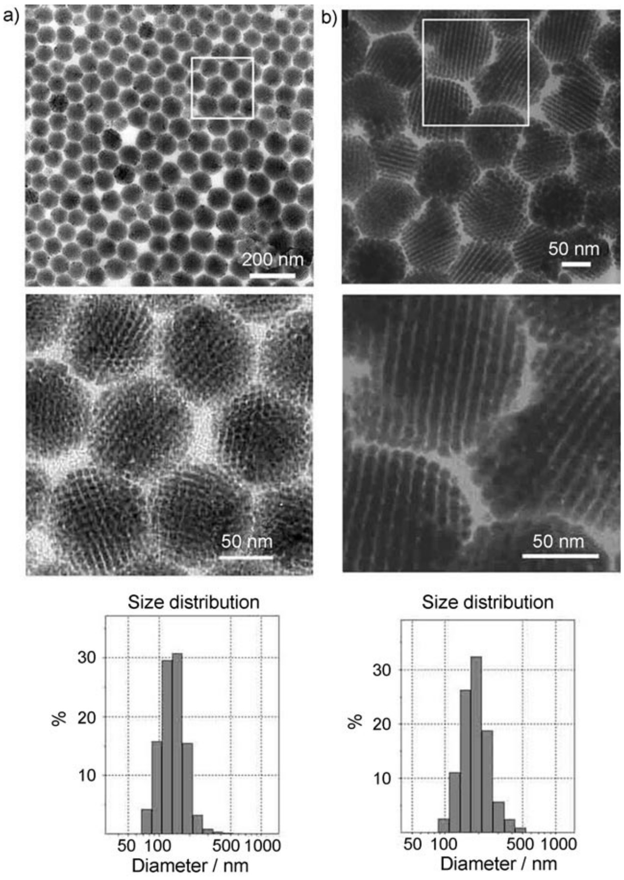

Figure 2. Typical TEM images (top), high-resolution images (middle), and DLS size-distribution diagrams (bottom) of $BaCrO_4$ (a) and Ag_2Se (b) colloids.

CTAB as the surfactant (see Figure S3 e in the Supporting Information). The interparticle gap estimated from Figure 2 b and from Figure S3 d in the Supporting Information is about 2.6 nm for the Ag_2Se assembly, which is smaller than the double thickness of a contracted ligand monolayer (octadecyl amine 2.3 nm), which is similar to the result of the $BaCrO_4$ colloidal spheres.

The above results show that this EBS strategy is a simple and facile synthetic method for preparing colloidal spheres from NC building blocks. This approach may open the way for the preparation of different kinds of 3D inorganic colloidal spheres from NCs. Figure 3 shows a series of typical TEM images of colloidal spheres assembled from different representative well-dispersed NCs, such as CdS, PbS, Fe_3O_4, ZrO_2, $NaYF_4$, Bi_2S_3 nanoplates, $PbSeO_3$ nanorods, and LaF_3 nanoplates, through this EBS approach. The diameters of these colloidal spheres ranged from 50 nm to 200 nm, depending on the size of the microemusion droplets formed for a given set of designed experimental conditions. From the typical high-resolution TEM images, it is seen that the NCs do not sinter into larger units (see Figures S4 and S5 in the Supporting Information). It can be clearly seen that some of these 3D colloidal spheres can self-assemble into ordered two-dimensional arrays on the TEM grid, which indicates that these spherical assemblies may serve as mesoscale building blocks for more complex macroscopic functional architectures.

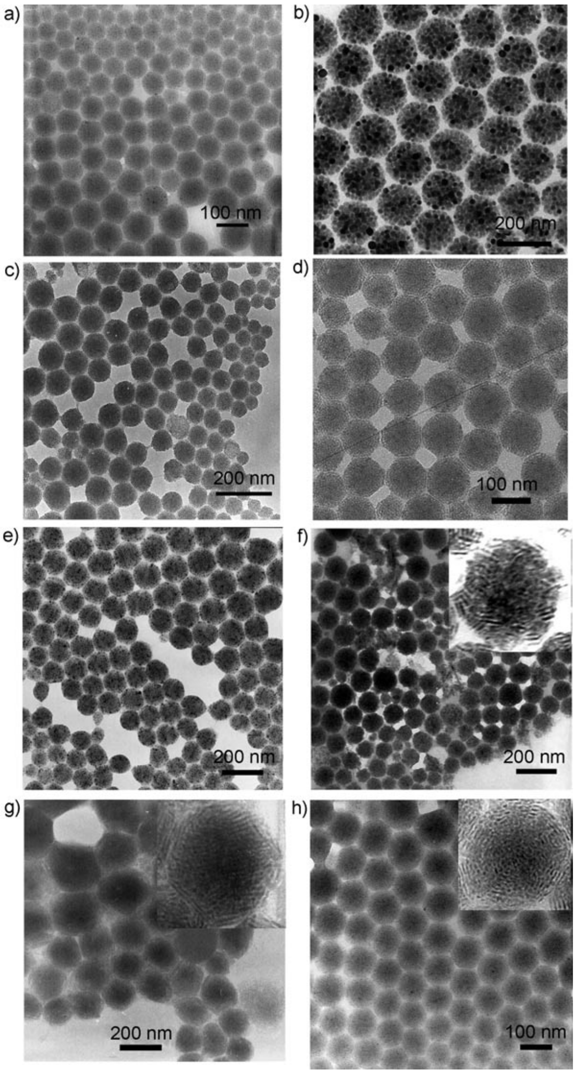

Figure 3. TEM images of representative colloidal spheres assembled from different NCs. a) CdS, b) PbS, c) Fe_3O_4, d) ZrO_2, e) $NaYF_4$, f) Bi_2S_3 nanoplates, g) $PbSeO_3$ nanorods, h) LaF_3 nanoplates.

The high-resolution TEM images (inset in Figure 3 f, g) show that these two types of colloidal spheres consist of Bi_2S_3 nanoplates and $PbSeO_3$ nanorods, respectively. The corresponding high-resolution TEM image (inset in Figure 3 h) of the LaF_3 nanoplate assembly shows thin platelike aggregates of 3D colloidal spheres. This assembly is constructed from a layer-by-layer array of uniformly sized LaF_3 nanoplates that are separated by an interlayer spacing of about 2.2 nm, consistent with the interparticle gap in the $BaCrO_4$ 3D ordered colloid. Viewed within the spherical assembly, the LaF_3 NCs are rectangular in shape with mean dimensions of about 8.0 nm and 1.5 nm. But the NCs are nearly round in shape with a uniform diameter of about 8.0 nm when viewed on the copper grid (as reported in our previous report[12]). The plate diameter measured for the NCs on the copper grid was commensurate with the longer side of NCs in the 3D assembly, suggesting that the larger side faces were preferentially juxtaposed in the 3D layer-by-layer array. The absence of layer-by-layer arrays in the Bi_2S_3 spherical assembly is probably due to the decreased mobility of the NCs, as they have a larger diameter than the LaF_3 plates. The larger diameter hinders reorientation of the NCs during drying, and they can't assemble into the layer-by-layer arrays. These results demonstrate that the EBS approach can be used to assemble a variety of shapes of NCs such as nanoparticles, nanorods, and nanoplates.

The diameter of the colloidal spheres can be controlled by adjustment of the emulsification process, NC concentration in the oil phase, surfactant concentration in the water phase, and oil-to-water ratio. For example, CdS assemblies with a diameter larger than 500 nm were obtained by strong mechanical stirring (greater than 1500 rpm), and spheres with a diameter smaller than 300 nm were obtained by sonication emulsification. The CdS assembly diameter increased with increasing NC concentration in the oil phase, decreasing surfactant concentration in the water phase, or increasing oil-to-water ratio (see Table S1 and Figure S9 in the Supporting Information). Changing the surfactant allows facile control of the assemblies' surface charge and functionality. In our method, either the cationic surfactant CTAB, anionic SDS, and even nonionic P123 (a triblock copolymer ($EO_{20}PO_{70}EO_{20}$, $M_r = 5800$, Aldrich)) can be used to form 3D spherical assemblies.

In summary, a general emulsion-based bottom-up self-assembly (EBS) approach was developed to assemble various kinds of NC building blocks with different composition, shape, size, and surfactant ligands into 3D colloidal spheres. The composition, size, and surface charge of the 3D colloidal spheres were controlled by rationally designing the experimental conditions. This EBS approach can be expected to open the way to new types of 3D colloidal spheres from nanocrystal building blocks, which may serve as mesoscale building blocks for constructing integrated architectures or devices for fundamental study and practical applications in nanoscience and nanotechnology.

Experimental Section

In a general preparation of water-dispersed 3D colloidal spheres from oil-dispersed NCs, SDS (28 mg) was added to deionized water (10 mL). A solution containing $BaCrO_4$ NCs (5 mg) in cyclohexane (1 mL) was added to the aqueous solution (the NC concentration of the stock dispersions was determined by drying and weighing, and then correlating the concentrations with the absorption of the dispersions by absorption spectral analysis). This system was then emulsified by ultrasonic treatment. The cyclohexane was removed by heating at 70 °C with constant stirring for 4 h to assemble the NCs into 3D spheres. After the reaction was cooled to room temperature, the products were collected and purified by repeated centrifugation and were redispersed. The final products were stored in water. The optical images resulting from this approach are listed in Figure S1 in the Supporting Information. The procedures for the other microemulsion-based bottom-up self-assemblies were similar to this one, except that the NC type, NC concentration, or surfactant type was altered.

The size and morphology of the products were determined at 200 kV with a Hitachi H-1200 transmission electron microscope (TEM) and a JEOL JEM-2010F high-resolution transmission electron microscope (HRTEM). Samples were prepared by placing a drop of a water dispersion of assembly spheres on the surface of a copper grid. The size distributions and zeta potentials of the 3D colloidal spheres were determined with a Zetasiezer 3000HS.

Received: March 29, 2007

Keywords: colloids · emulsion-based methods · nanostructures · self-assembly · surfactants

---

[1] a) J. M. Phillips, *MRS Bull.* **2006**, *31*, 44–49; b) G. M. Whitesides, *Sci. Am.* **1995**, *273*, 146–149; c) J. M. Lehn, *Science* **2002**, *295*, 2400–2403.

[2] a) Y. N. Xia, G. M. Whitesides, *Annu. Rev. Mater. Sci.* **1998**, *28*, 153–184; b) P. Yang, G. Wirnsberger, H. C. Huang, S. R. Cordero, M. D. McGehee, B. Scott, T. Deng, G. M. Whitesides, B. F. Chmelka, S. K. Buratto, G. D. Stucky, *Science* **2000**, *287*, 465.

[3] a) Y. Yin, A. P. Alivisatos, *Nature* **2005**, *437*, 664–670; b) Y. Huang, C. M. Lieber, *Pure Appl. Chem.* **2004**, *76*, 2051–2068; c) Y. Cui, M. T. Bjork, J. A. Liddle, C. Sonnichsen, B. Boussert, A. P. Alivisatos, *Nano Lett.* **2004**, *4*, 1093–1098.

[4] a) C. J. Kiely, J. Fink, M. Brust, D. Bethell, D. J. Schiffrin, *Nature* **1998**, *396*, 444–446; b) A. K. Boal, F. Ilhan, J. E. DeRouchey, T. Thurn-Albrecht, T. P. Russell, V. M. Rotello, *Nature* **2000**, *404*, 746–748; c) A. Courty, A. Mermet, P. A. Albouy, E. Duval, M. P. Pileni, *Nat. Mater.* **2005**, *4*, 395–398.

[5] C. B. Murray, C. R. Kagan, M. G. Bawendi, *Science* **1995**, *270*, 1335–1338.

[6] A. M. Kalsin, M. Fialkowski, M. Paszewski, S. K. Smoukov, K. J. M. Bishop, B. A. Grazybowski, *Science* **2006**, *312*, 420–424.

[7] E. Rabani, D. R. Reichman, P. L. Geissler, L. E. Brus, *Nature* **2003**, *426*, 271–274.

[8] C. B. Murray, C. R. Kagan, M. G. Bawendi, *Science* **1995**, *270*, 1335–1338.

[9] a) W. Shenton, D. Pum, U. B. Sleytr, S. Mann, *Nature* **1997**, *389*, 585–587; b) P. V. Braun, P. Osenar, S. I. Stupp, *Nature* **1996**, *380*, 325–328; c) M. Li, H. Schnablegger, S. Mann, *Nature* **1999**, *402*, 393–395.

[10] a) F. X. Redl, K. S. Cho, C. B. Murray, S. O'Brien, *Nature* **2003**, *423*, 968–971; b) E. V. Shevchenko, D. V. Talapin, N. A. Kotov, S. O'Brien, C. B. Murray, *Nature* **2006**, *439*, 55–59; c) S. H. Sun, C. B. Murray, D. Weller, L. Folks, A. Moser, *Science* **2000**, *287*, 1989–1992.

[11] M. M. Maye, S. C. Chun, L. Han, C. J. Zhong, D. Rabinovich, *J. Am. Chem. Soc.* **2002**, *124*, 4958–4959.

[12] X. Wang, J. Zhuang, Q. Peng, Y. D. Li, *Nature* **2005**, *437*, 121–124.

[13] J. P. Ge, W. Chen, L. P. Liu, Y. D. Li, *Chem. Eur. J.* **2006**, *12*, 6552–6558.

[14] Z. Y. Huo, C. Chen, Y. D. Li, *Chem. Commun.* **2006**, *33*, 3522–3524.